*Journal of Power Sources*, *30* (1990) 143 - 152 

# INSERTION MECHANISM OF THE LEAD DIOXIDE ELECTRODE

H. W. UHLIG

*VEB Berliner Akkumulatoren und Elementefabrik, Wilhelminenhofstrasse 68/69, 1160 Berlin (G.D.R.)*

## Introduction

Both an insertion mechanism (eqn. (1)) and a solution mechanism (eqn. (2)) have been investigated for $PbO_2$, *i.e.*,

$$PbO_2 + xH^+ + xe^- \longrightarrow H_xPbO_2 \quad (1)$$

$$PbO_2 + H^+ + 2e^- \longrightarrow HPbO_2^- \quad (2)$$

A detailed understanding of the insertion conditions is important in order to achieve improvements in the theory of the $PbO_2$ electrode. In recent years, a number of theories have been developed for special insertion compounds such as $H_xMnO_2$, $Li_xTiO_2$, and $Li_xV_2O_5$. These theories show good agreement with experimental results, but differ in basic assumptions. The aim of the work reported here is first to classify the insertion compounds into typical groups and then to compare these groups in order to determine the characteristic parameters of the insertion mechanism. The results are applied to the $PbO_2$ electrode.

Insertion theories describe the dependence of the equilibrium voltage, $\varepsilon$, on the degree of insertion, $x$, using parameters such as repulsive interaction energy ($E_{rep}$), lattice expansion energy ($E_{exp}$), electron chemical potential ($\mu_e$), and contribution entropy ($\Delta S$), as shown in Table 1. These functions can be expressed in the form

$$\varepsilon = (\varepsilon^\circ + RT/F \ln(1 - x/x)) + F(x) \quad (3)$$

The first two terms on the right-hand side of eqn. (3) are commonly used in all theories and are, respectively, the normal voltage and the contribution entropy of the inserted pair, cation/electron. The third term considers the various parameters that are used in different ways in the particular theories as seen in Table 1.

Three equations have been derived [1 - 9] to describe the $\varepsilon/x$ functions:

$$\varepsilon = \varepsilon^\circ + 2RT/F \ln(1 - x/x) \quad (4)$$

$$\varepsilon = \varepsilon^\circ + RT/F \ln(1 - x/x) + k(x) \quad (5)$$

$$\varepsilon = \varepsilon^\circ + RT/F \ln(1 - x/x) + k(x - 0.5) \quad (6)$$

0378-7753/90/$3.50 

TABLE 1

$\varepsilon/x$ functions

| Compound | Function of $F(x)$ | Energy | Ref. |
|---|---|---|---|
| | $\varepsilon = \varepsilon^\circ + RT/F \ln(1 - x/x) + F(x)$ | | |
| $Li_xTiS_2$ | $6Ux$ | $E_{rep}$ | 1, 2 |
| | $z\omega x + F(d\mu_e/dx) + B(dc/dx)$ | $\mu_e$, $E_{rep}$, $E_{exp}$ | 3 |
| | $k(x - 0.5)$ | $E_{rep}$ | 4 |
| $Li_xV_2O_5$ | $zE(x/F)$ | $E_{rep}$ | 5 |
| | $kx$ | $E_{rep}$ | 6 |
| $H_xMnO_2$ | $RT/F \ln(1 - x/x)$ | $\mu_e$ | 7 |
| | $RT/F \ln(1 - x/x)$ | $\Delta S_{mix}$ | 8 |
| | $\Phi(1 - x)$ | $E_{rep}$ | 9 |

## Experimental

$\varepsilon/x$ curves for insertion compounds have been selected from experimental results that have been reported in the literature. The insertion compounds are categorized into four groups, as expressed by the characteristic $\varepsilon/x$ curves, see Figs. 1 - 4. The compounds are listed in Table 2.

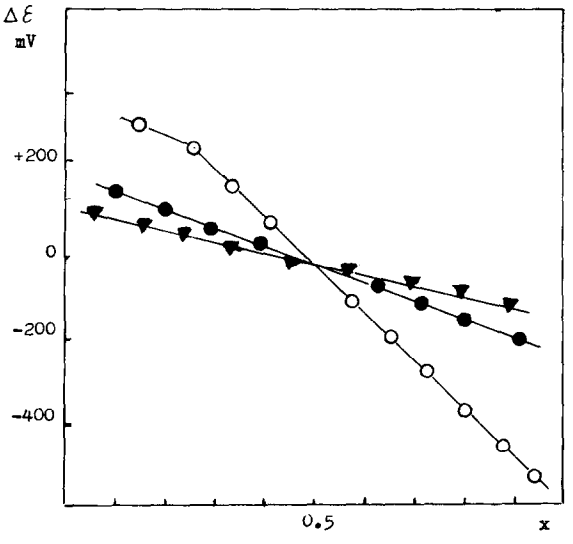


Fig. 1. $\varepsilon/x$ curves. ●, $Li_xTiS_2$ [10]; ○, $Li_xTaS_2$ [11]; ▼, $Li_xVS_2$ [12].

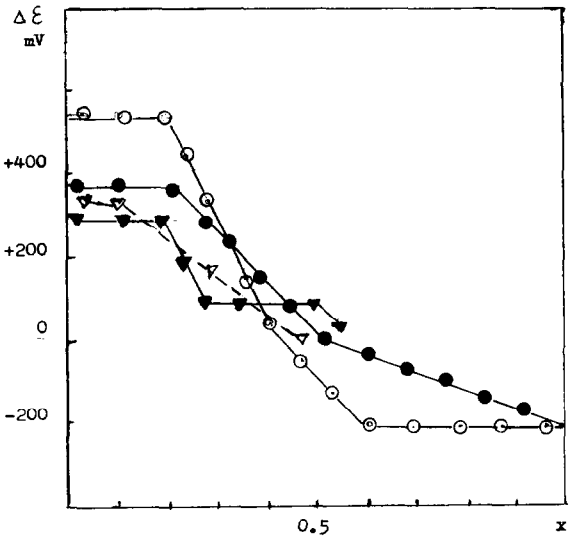


Fig. 2. $\varepsilon/x$ curves. ●, $H_xMoO_3$ [13]; ○, $Li_xMoO_3$ [14]; ▽, $H_xWO_3$ [15]; ▼, $Li_xV_2O_5$ [16, 6].

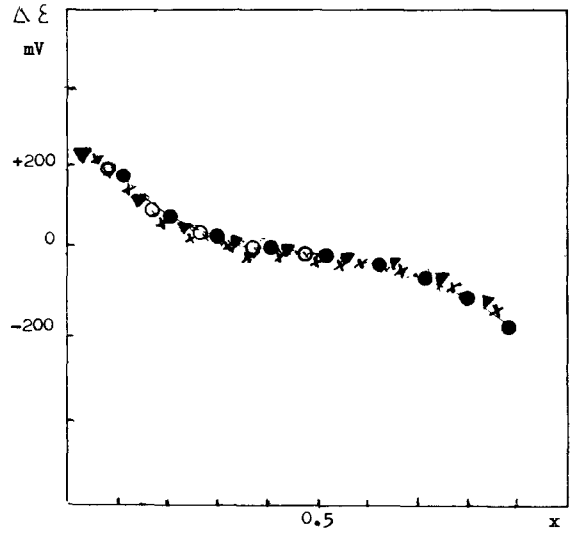


Fig. 3. $\varepsilon/x$ curves. ●, $H_xMnO_2$ [17]; ○, $H_xNiO_2$ [18]; ×, $K_3Fe(CN)_6$ [19]; ▼, polyvinylferrocene [20].

TABLE 2

Classification of insertion compounds by $\varepsilon/x$ functions

| | |
|---|---|
| Group 1 | $Li_xTiS_2$ $Li_xTaS_2$ $Li_xVS_2$ |
| Group 2 | $H_xMoO_3$ $Li_xMoO_3$ $Li_xV_2O_5$ $H_xWO_3$ |
| Group 3 | $H_xMnO_2$ $H_xNiO_2$ $K_3Fe(CN)_6$ Polyferrocene |
| Group 4 | $Li_xMnO_2$ $Li_xTiO_2$ $Li_xCuO$ $Na_xWO_3$ |

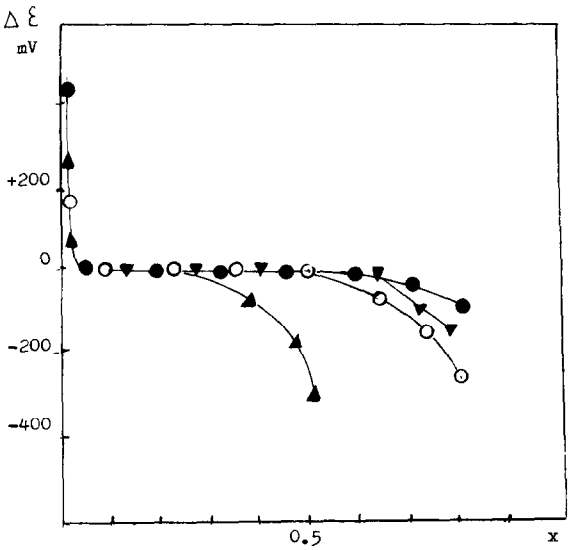


Fig. 4. $\varepsilon/x$ curves. ●, $Li_xMnO_2$ [21]; ▲, $Li_xTiO_2$ [22]; ○, $Li_xCuO$ [23]; ▼, $Na_xWO_3$ [24].

## Discussion

Four characteristic $\varepsilon/x$ curves can be derived from Figs. 1 - 4; these are summarized in Fig. 5. The curves will be discussed by comparison of the energy, $E_{el}$, calculated by:

$$E_{el} = -F \int_{x=0}^{x=1} \varepsilon(x) \cdot dx \tag{7}$$

and the insertion enthalpy $\Delta H_i$. The latter can be obtained from calorimetric measurements and eqn. (8) [10, 11, 15, 16, 24]. The insertion enthalpy corresponds to the Gibbs energy, $\Delta G$, because $T\,\Delta S$ can be neglected

$$\Delta G = \Delta H_i = \mu_{AMO_n} - (\mu_A + \mu_{MO_n})$$
$$T\Delta S \ll \Delta H; \quad (A = H^+, Li^+) \tag{8}$$

Differences between $E_{el}$ and $\Delta G$ are termed the insertion energy, $E_i$.

The $\varepsilon/x$ curve of Group 1 compounds shows a constant decrease in the voltage. The curve is described by:

$$\varepsilon = \varepsilon^\circ + k(x - 0.5) \tag{9}$$

This relationship is derived from eqn. (6), neglecting the term $RT/F \times \ln(1 - x/x)$ because the influence of the latter is small, and a deviation from the straight lined $\varepsilon/x$ curve is not witnessed in any of the experimental

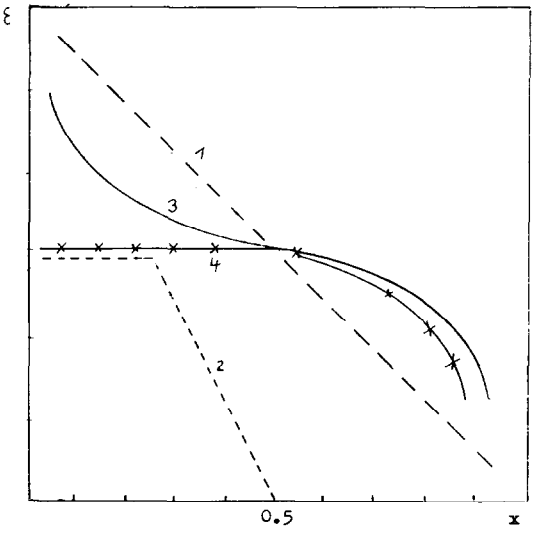


Fig. 5. Typical $\varepsilon/x$ curves for insertion compounds. ——, Group 1; – – – –, Group 2; ——, Group 3; –x–x–, Group 4.

curves. The electrical energy and the Gibbs energy are very similar, as shown in Table 3. Therefore:

$$E_{el} = -\varepsilon^{\circ}F = \Delta G \tag{10}$$

The typical $\varepsilon/x$ curve of the Group 2 compounds is presented in Fig. 6 in a more detailed form. The curve has an initial region with a constant voltage level corresponding to the normal voltage, and a second region in which the voltage decreases linearly up to $0.5x$. As is shown in Fig. 6, extrapolation of the $\varepsilon/x$ curve to $x = 0.5$ and $x = 0$ yields the normal voltage $\varepsilon^{o,x}$ and the initial voltage $\varepsilon^{x}_{x_0}$, respectively (for $V_2O_5$, the extrapolation includes two voltage steps). From curve 1 (which results from the extrapolated values) the

TABLE 3

Comparison of electrical energy, $E_{el}$, and insertion enthalpy, $\Delta H_i$

| Compound | $-\Delta H_i$ (kJ mol$^{-1}$) | $-E_{el}$ (kJ mol$^{-1}$) |
|---|---|---|
| $Li_xTiS_2$ | 210 | 212 |
| $Li_xTaS_2$ | 211 | 220 |
| $Li_xVS_2$ | 220 | 230 |
| $H_xMoO_3$ | 60 | 55 |
| $Li_xMoO_3$ | 284 | 279 |
| $Li_xV_2O_5$ | 328 | 320 |

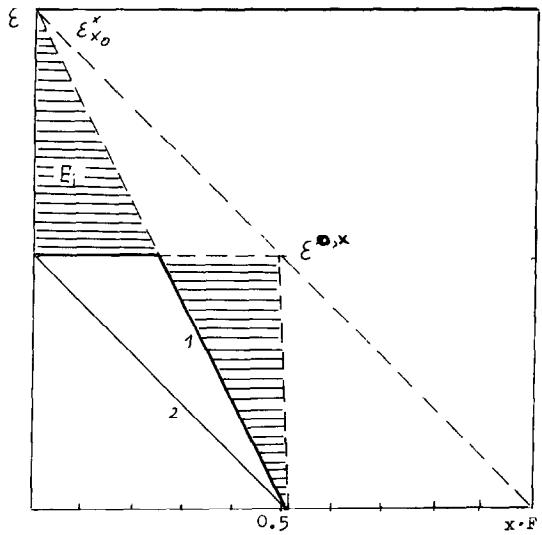


Fig. 6. Scheme of typical $\varepsilon/x$ curve of Group 2 insertion compound.

electrical energy, $E^x_{el}$, can be calculated that corresponds with the insertion enthalpy for $x = 0.5$, as shown in Table 3, *i.e.*,

$$E^x_{el} = -1/2(\varepsilon^{o,x} - \varepsilon^x_{x_0})0.5F = -\varepsilon^{o,x}0.5F = \Delta H_{i/2} \tag{11}$$

Figure 6 shows that the real electrical energy, $E_{el}$, differs from eqn. (11) by the value $E_i$ which is calculated from the area above the constant voltage region. Thus, we conclude that the constant voltage region results from an energy that is necessary to break bondings in the host lattice and is not caused by an heterogeneous phase, as is normally assumed.

The $\varepsilon/x$ function of the extrapolated curve is

$$\varepsilon = \varepsilon^\circ + k(2x - 0.5) \tag{12}$$

$$k = 2\Delta H_i/F \tag{13}$$

Unlike the functions of Group 1 compounds, $k$ depends on the insertion enthalpy of the compounds. Both Group 1 and Group 2 compounds have layer structures. Thus, the bonding energy between the layers of M–O compounds must be stronger than that in M–S compounds. The reason for the difference could be the stronger covalent M–S bonding [25].

The $\varepsilon/x$ curve for $H_xWO_3$ differs from that of the other compounds of the Group (see curve 2, Fig. 6). The curve is described by:

$$\varepsilon = \varepsilon^\circ - kx \tag{14}$$

Unlike the other compounds, $WO_3$ has a framework structure.

Various compounds are represented by $\varepsilon/x$ curve 3 in Fig. 5. The compound in the Group that has been investigated most is $MnO_2$. By contrast

to $WO_3$, hydrogen insertion does not occur in channels of the unhydrated oxide. The hydrogen insertion requires OH groups that are bound on particular sites in the channels of $\gamma$-$MnO_2$ [26]. The OH groups are incorporated in the lattice during the electrolytic preparation [27]. The hydration is associated with an enthalpy enhancement [28, 29], *i.e.*,

$$MnO_2 + mH_2O \xrightarrow{\Delta H_m} MnO_2 \cdot mH_2O \tag{15}$$

Thus, $\Delta H_m$ can be considered to be an insertion energy that is contributed by a "pre-insertion step":

$$E_{el} = -\varepsilon^\circ F = \Delta H_i(H_x MnO_2) + \Delta H_m \tag{16}$$

The $\varepsilon/x$ curve for $H_xNiO_2$ is in good agreement with that of $H_xMnO_2$ [18, 30]. $NiO_2$, however, has a layer structure and the OH groups are situated between the layers. Unlike $NiO_2$, $\delta$-$MnO_2$ (which also has a layer structure containing $OH^-$ groups between the layers) does not exhibit hydrogen insertion [31, 32]. Therefore, it is concluded that the nature of the OH bonding that can be realized in different structural forms is the characterizing criterion for the oxides of Group 3. Equation (4) was derived for $MnO_2$ assuming independently inserted protons and electrons on particular sites in the lattice [7, 8] and an additional contribution to the entropy, namely, an electron chemical potential, $\mu_e$:

$$\varepsilon = \varepsilon^\circ + RT/F \ln(1 - x/x) + \mu_e \tag{17}$$

There are Fe atoms situated analogous to the MnO–OH groups in the compounds Prussian blue and polyferrocene. These Fe atoms are connected to groups having free electrons or conjugated $\pi$-electrons, *i.e.*,

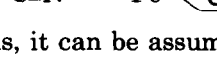

Thus, it can be assumed that insertion to particular positions is a characteristic for all Group 3 compounds, and eqn. (4) represents the common $\varepsilon/x$ function for the Group. The insertion mechanisms can be described by the equations:

$$MO_{(2-m)}(OH)_{2m} + xH^+ + xe^- \rightarrow H_xMO_{(2-m)}(OH)_{2m} \tag{18}$$

$$(M - \otimes)_n + xA^+ + xe^- \longrightarrow A_x^+ (M - \otimes)_n \tag{19}$$

(A = alkali, $\otimes$ = energetically particular positions with free electrons or $\pi$-electrons).

The typical $\varepsilon/x$ curve of Group 4 compounds shows: (i) an initial region with a constant voltage level similar to that of Group 2 compounds, but prolonged to $x = 0.5$; (ii) a second region in which the curve corresponds principally to that of Group 3 compounds. The compounds of Group 4 are lithium-inserted metal dioxides having a framework structure. It is assumed that the first region is defined by an insertion energy according to Group 2. As shown in Table 4, the compounds of Group 4 differ from those of other groups by having very high values for the diffusion coefficient. It is remarkable

TABLE 4

Diffusion coefficients of inserted cations

| Group | Compound | $D$ ($cm^2\ s^{-1}$) | Ref. |
|---|---|---|---|
| 2 | $Li_xMoO_3$ | $3 \times 10^{-9}$ | 24 |
| | $Li_xV_2O_5$ | $9 \times 10^{-9}$ | 24 |
| 3 | $H_xMnO_2$ | $6 \times 10^{-10}$ | 33 |
| | $H_xPbO_2$ | $1 \times 10^{-7}$ | 34 |
| | $H_xNiO_2$ | $3 \times 10^{-10}$ | 30 |
| 4 | $Li_xMnO_2$ | $3 \times 10^{-11}$ | 24 |
| | $Li_xTiO_2$ | $3 \times 10^{-13}$ | 35 |

that lithium insertion proceeds in the channels of the rutile-type oxides $\beta$-$MnO_2$, $TiO_2$ and $IrO_2$, whilst hydrogen insertion does not. Therefore, steric conditions are not the reason for the prevention of hydrogen insertion.

On the basis of the above conditions for the insertion mechanism, an investigation has been made of $PbO_2$. It is expected that $PbO_2$ can be classified in Group 3 and that it is similar to $MnO_2$ in many aspects. Therefore, it should be useful to compare these two oxides. Three pairs of oxides are considered:

*(i) $\beta$-$MnO_2$ and $\beta$-$PbO_2$(chem.).* These are stoichiometric compounds and are isostructural with a framework structure of the rutile-type formed by $MO_6$-octahedra sharing one edge.

*(ii) $\delta$-$MnO_2$ and $\alpha$-$PbO_2$(chem.).* These are non-stoichiometric compounds containing OH groups and are characterized by the formulae:

$Na_{0.3}MnO_{1.93}\cdot 0.6H_2O$

$PbO_{(1.83-1.93)}\cdot(0.1-0.3H_2O)$

The structures are different. $MO_6$ octahedra, sharing one edge, form layers in the case of $MnO_2$ and a framework structure in the case of $PbO_2$.

*(iii) $\gamma$-$MnO_2$ and $\alpha$-$PbO_2$(electrochem.).* These are non-stoichiometric oxides of the composition:

$MnO_{1.96}\cdot 0.23H_2O$

$PbO_{1.98}\cdot(0.2-0.3)H_2O$

Their crystal structures are orthorhombic and are derived from the rutile type.

The assumptions adapted in the insertion mechanism are, first, a lattice that is suitable for insertion by gaps or channels and, second, a high mobility for the inserted cations. The first assumption is applicable to all three pairs of oxides, but the second assumption is only applicable to the third pair. The hydrogen ions move via a jumping mechanism involving OH groups [34, 36] and thus the insertion process only occurs in the third pair of oxides. The latter, $\gamma$-$MnO_2$ and $\alpha$-$PbO_2$(electrochem.), differ from the other oxides in

several important features: the OH groups are incorporated in the lattice by an electrochemical process (hydrolysis and crystal growth during electrolysis [27, 37]). The $MO_6$ octahedra share more than one edge. The M–O bonding is strongly covalent [38]. $\gamma$-$MnO_2$ and $\alpha$-$PbO_2$ also differ in the structure of the channels. The $MnO_2$ lattice consists of double $MnO_6$ octahedra chains forming $1 \times 2$ channels [31]. The lattice of $PbO_2$ has $1 \times 1$ channels, similar to $\beta$-$PbO_2$ but is arranged in zig-zag chains. Therefore, it is concluded that the influence of the crystal structures on the mobility of the hydrogen ions depends upon the nature of the PbO bonding caused by the crystal structure.

## Conclusions

(i) It is assumed that two basic types of insertion exist that are characterized by different $\varepsilon/x$ functions:

- insertion in gaps of layer-structured metal dichalcogenides having insertion sites of equal energy
- insertion in channels or gaps of framework or layer-structured compounds that have energetically favoured positions for the inserted cations and electrons. Such positions may be MO groups ordered with a particular type of vacancies or metal atoms connected with groups having free electrons or conjugated electrons.

(ii) The basic types are characterized by strongly covalent bonding in the host lattice.

(iii) Insertion types that require insertion energy to break the bonds between the respective layers in the channels are derived from the basic types. Initial regions of constant voltage, that are usually due to heterogeneous phases, result from the insertion energy.

(iv) $\alpha$-$PbO_2$(electrochem.) is an insertion compound of the second basic type related to $\gamma$-$MnO_2$.

(v) The mobility of hydrogen ions in the channels of the $PbO_2$ lattice is dependent upon the nature of the Pb–O bonding that is caused by particular sites in the crystal structure.

## List of symbols

| | |
|---|---|
| $\varepsilon$ | Electrode voltage |
| $\varepsilon^\circ$ | Normal voltage |
| $R$ | Gas constant |
| $F$ | Faraday constant |
| $E_i$ | Insertion energy |
| $E_{el}$ | Electrical energy |
| $E_{rep}$ | Repulsive interaction energy |
| $E_{exp}$ | Lattice expansion energy |
| $\mu$ | Chemical potential |

$G$ Gibbs energy
$H_i$ Insertion enthalpy
$S$ Entropy
$H_m$ Hydration enthalpy
$x$ Degree of insertion

## References


1 A. J. Berlinski, W. R. Unruh, W. R. McKinnon and R. R. Hearing, *Solid State Commun., 31* (1979) 135.
2 S. Sinha and D. W. Murphi, *Solid State Ionics, 20* (1986) 81.
3 A. S. Nagelberg and W. L. Worell, *J. Solid State Chem., 38* (1981) 321.
4 S. Atlung, B. Zachau-Christiansen, K. West and T. Jacobsen, *J. Electrochem. Soc., 131* (1984) 1200.
5 A. Hammouche and A. Hammou, *Electrochim. Acta, 32* (1987) 1451.
6 Y. Muranushi, T. Miura, T. Kishi and T. Nagai, *J. Power Sources, 20* (1987) 187.
7 S. Atlung and J. Jacobson, *Electrochim. Acta, 26* (1981) 1447.
8 W. C. Maskell, J. E. A. Shaw and F. L. Tye, *Electrochim. Acta, 28* (1983) 231.
9 P. Ruetschi, *J. Electrochem. Soc., 135* (1988) 2657.
10 W. B. Johnson and W. L. Worell, *J. Electrochem. Soc., 133* (1986) 1966.
11 J. R. Dahn and W. R. McKinnon, *J. Electrochem. Soc., 131* (1984) 1823.
12 M. S. Wittingham, *Prog. Solid State Chem., 12* (1978) 41.
13 R. Schöllhorn, *Angew. Chem., 92* (1980) 1015.
14 G. Pistoia, F. Rodante and M. Tocci, *Solid State Ionics, 20* (1986) 25.
15 P. G. Dickens, S. J. Hibble and M. A. Steers, *Solid State Ionics, 20* (1986) 209.
16 M. Yoshizawa, M. Takashi and T. Tomiya, *Denki Kagaku, 55* (1987) 756.
17 D. M. Holton, W. C. Maskell and F. L. Tye, *14th Int. Power Sources Symp., Brighton, 1984,* No. 17, S.247.
18 F. Jones and W. F. K. Wynn-Jones, *Trans. Faraday Soc., 52* (1956) 1260.
19 T. Ohzuku and K. Sawai, *J. Electrochem. Soc., 123* (1985) 2828.
20 C. Iwakura, T. Kawai, M. Nojima and H. Yoneyama, *J. Electrochem. Soc., 134* (1987) 791.
21 J. C. Nardi, *J. Electrochem. Soc., 132* (1985) 1787.
22 T. Ohzuku, Z. Takehara and S. Yoshizawa, *Electrochim. Acta., 24* (1979) 2.
23 P. Novak, B. Klapste and P. Podhajecky, *J. Power Sources, 15* (1985) 101.
24 P. C. Dickens and G. J. Reynolds, *Solid State Ionics, 5* (1981) 331.
25 Cl. Ritter, *Z. Phys. Chem.(N.F.), 151* (1987) 51.
26 W. C. Maskell, J. E. Shaw and F. L. Tye, *Electrochim. Acta, 28* (1983) 225.
27 J. Y. Welsh, *Electrochem. Technol., 5* (1967) 504.
28 E. Preisler, *J. Appl. Electrochem. 66* (1976) 311.
29 H. W. Uhlig, *J. Power Sources, 23* (1988) 295.
30 G. Halpert, *J. Power Sources, 12* (1984) 177.
31 R. G. Burns and V. M. Burns, *Proc. $MnO_2$ Symp., Tokyo, 1980,* Vol. 2, p. 97.
32 D. M. Holton, W. F. Maskell and F. L. Tye, *14th Int. Power Sources Symp., Brighton, 1984,* No. 17, p. 247.
33 H. Kahre, J. Delaid, J. Guitton and J. P. Cohen-Addad, *Surf. Technol., 16* (1982) 331.
34 J. R. Gavarri, P. Garnier, P. Boher, A. J. Dianoux, G. Chedeville and B. Jocq, *J. Solid State Chem., 75* (1988) 251.
35 K. Kanamura, K. Yuasa and Z. Takehara, *J. Power Sources, 20* (1987) 2391.
36 P. Ruetschi, *J. Electrochem. Soc., 131* (1984) 2737.
37 R. J. Hill and M. R. Houchin, *Electrochim. Acta, 30* (1985) 559.
38 G. M. Clark, *The Structures of Non-molecular Solids,* Applied Science Publishers, London, 1972.